

# Dissolution Behaviour of NbC during Slab Reheating

Hongyeob LEE,<sup>1)</sup> Kyong-Su PARK,<sup>2)</sup> Jung Hyeung LEE,<sup>2)</sup> Yoon-Uk HEO,<sup>1)</sup> Dong-Woo SUH<sup>1)\*</sup> and Harshad Kumar Dharamshi Hansraj BHADESHIA<sup>1,3)</sup>

1) Graduate Institute of Ferrous Technology, POSTECH, Pohang, Kyeongbuk, 790-784 Republic of Korea.

2) Technical Research Laboratories, POSCO, Pohang, Kyeongbuk, 790-785 Republic of Korea.

3) Materials Science and Metallurgy, University of Cambridge, 27 Charles Babbage Road, Cambridge, CB3 0FS, U.K.

(Received on November 22, 2013; accepted on April 7, 2014)

It is common practice to reheat continuously cast slabs prior to hot-rolling. Here we examine the dissolution of niobium carbide precipitates present in the cast slabs, as a function of the temperature during heating at a typical rate. The initial condition of precipitates in slab is quantified with transmission electron microscopy. Kinetic simulations and interrupted quenching experiments indicate that the precipitates persist well beyond the equilibrium dissolution temperature. The coarsening of the precipitates during heating, as opposed to a general lowering in the mean size due to dissolution, occurs only at heating rates some two orders of magnitude slower than typical.

KEY WORDS: NbC; reheating; dissolution; steel; simulation.

## 1. Introduction

Microalloying using niobium, titanium or vanadium in low-carbon steels is a common feature of thermomechanically processed high-strength, low-alloy steels. By forming fine carbides, these elements can lead to a general refinement of the microstructure in the processed steel, and add to strength by precipitation hardening.<sup>1–6)</sup>

Steel manufacture often involves the continuous casting of slab, which is allowed to cool to ambient temperature, permitting the carbides to precipitate. When the system is ready to receive the steel for processing, the slab is reheated; the carbides then begin to dissolve and the rate of this process depends on the initial size distribution and number density of particles, so that the concentration of microalloying elements in solution during the initial stages of hot deformation can be affected by the dissolution process.

One approximation to the quantity of niobium precipitated at any time is to use the equilibrium solubility product or a phase diagram calculation capable of greater generality. However, there are experimental data to suggest that alloy carbides such as those of niobium can take a significant time to dissolve.<sup>7,8)</sup> Indeed, it is likely that there is a significant size distribution in the carbides so that the larger category should take a longer time to dissolve.<sup>9)</sup> There have been previous attempts to model the dissolution. One such method approximates the steel as a ternary Fe–Nb–C system from a thermodynamic point of view, but treating at the same time only the diffusion of niobium, and using a random walk solution for diffusion.<sup>7,10)</sup> More rigorous treatments<sup>11,12)</sup> account for capillarity, multicomponent diffusion in the con-

text of an Fe–Nb–C system, precipitation, coarsening and dissolution reactions but the analyses are limited to NbC in austenite whereas the reheating of a slab involves initially the heating of ferrite.

In this study, we report dissolution kinetics of NbC during the reheating of slab, taking into account the size distribution and transformation kinetics. The precipitation of NbC in cast slab is investigated quantitatively using transmission electron microscopy (TEM) to establish the initial condition prior to reheating. The dissolution kinetics of NbC during the reheating process are simulated using the software MatCalc which can handle the precipitation or dissolution process as a function of thermal history, thermodynamic and kinetic parameters for multicomponent and multiphase systems.<sup>13–15)</sup> Experimental verification of dissolution behaviour of NbC particles is conducted using transmission microscopy of samples quenched from a variety of temperatures during the heating process. The results are compared against expectations from equilibrium calculations.

## 2. Experimentals and Simulation

The chemical composition of the alloy investigated is 0.10C–0.89Mn–0.20Si–0.018Nb wt.%, without any titanium or vanadium so that the microalloying precipitates expected should be mainly NbC. Titanium in particular is known to stabilise NbC and hence retard its dissolution.<sup>16)</sup> A slab 700 mm wide and 250 mm in thickness was continuously cast in a pilot facility, and a specimen 150 × 100 × 10 mm was machined from the centre of the slab from which smaller specimens were extracted for microstructural analysis and heat treatment. The NbC was characterised in transmission microscopes using thin foil and carbon extraction replica specimens. The former were prepared by mechanical polish-

\* Corresponding author: E-mail: dongwool@postech.ac.kr  
DOI: <http://dx.doi.org/10.2355/isijinternational.54.1677>

ing to 100  $\mu\text{m}$  thickness, followed by electrochemical polishing in a 95% acetic acid and 5% perchloric acid solution at 20°C with constant voltage of 45 V. For carbon extraction replication, the surfaces of etched specimens were coated with carbon films, which were then detached in a mixture of 890 ml methanol, 100 ml acetyl acetone, and 10 g tetra methyl ammonium chloride at room temperature.

Dissolution of NbC during reheating of the slab was examined using simulated heat-treatment. Specimens with  $10 \times 10 \times 1$  mm were prepared and vacuum-sealed in quartz tubes to prevent oxidation during heat treatment. The specimen was heated at  $0.13^\circ\text{C s}^{-1}$ , which is typical practice of reheating process, to 1060°C, 1160°C and 1260°C, respectively, before interrupted quenching to room temperature. The undissolved NbC was characterised using thin foil specimens.

**Table 1.** Simulation parameters.

Austenite	Dislocation density, $10^{11} \text{ m}^{-2}$
	Grain size, $100 \mu\text{m}$
Ferrite	Dislocation density $10^{12} \text{ m}^{-2}$
	Grain size, $10 \mu\text{m}$

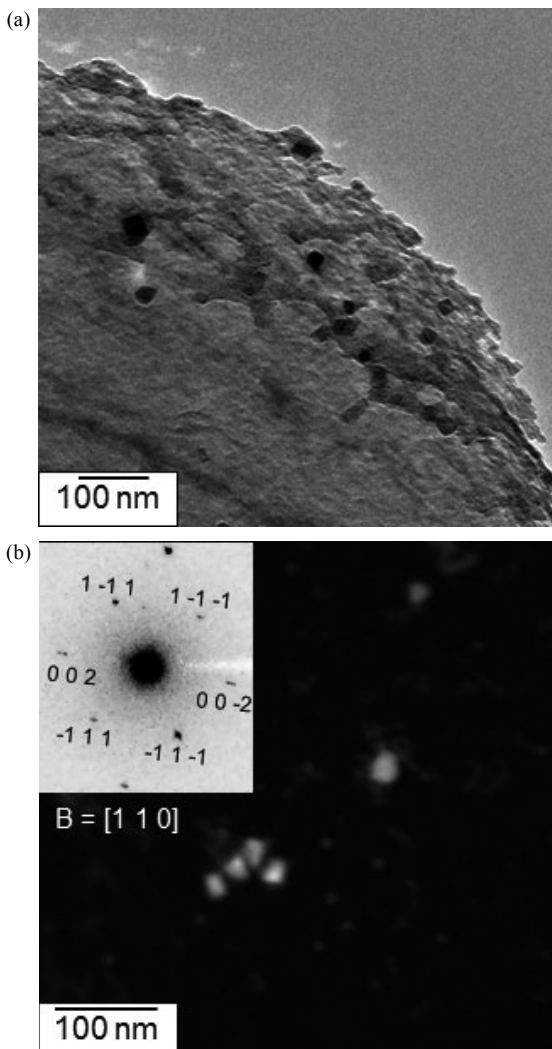


**Fig. 1.** NbC precipitates in the as-received steel. (a) Bright field image (thin foil), (b) dark field image (extraction replica).

The kinetics of NbC dissolution during heating were simulated with the MatCalc software (ver.5.52).<sup>13-15)</sup> In this method, the free energy of the system consisting of spherical particles in a matrix, and the dissipation rate of the free energy, are expressed as a function of chemical composition, interfacial energies and size of each particle, from which the growth or dissolution of particles with a given size distribution can be evaluated. The databases used are the MatCalc Fe thermodynamic database (ver.1.024) and the mobility database (ver.1.001). Lattice diffusivity of Nb in iron matrix was used for the simulation. The initial size distribution of NbC precipitation was measured using transmission electron microscopy, and the distribution was input into the software as an average size and standard deviation. Some 500 classes of NbC particles ranging from 2.6 nm to 26.8 nm were created to examine the dissolution behaviour. The initial fraction of NbC was assumed to correspond to equilibrium at room temperature. Other calculation conditions are listed in **Table 1**,<sup>17)</sup> but the nucleation of new particles is obviously absent in the dissolution simulation. Therefore the influence of grain size and dislocation density was insignificant in the present study and the simulations are therefore insensitive to the parameters listed in Table 1.

### 3. Results and Discussion

**Figures 1(a), 1(b)** show the NbC precipitation in the slab

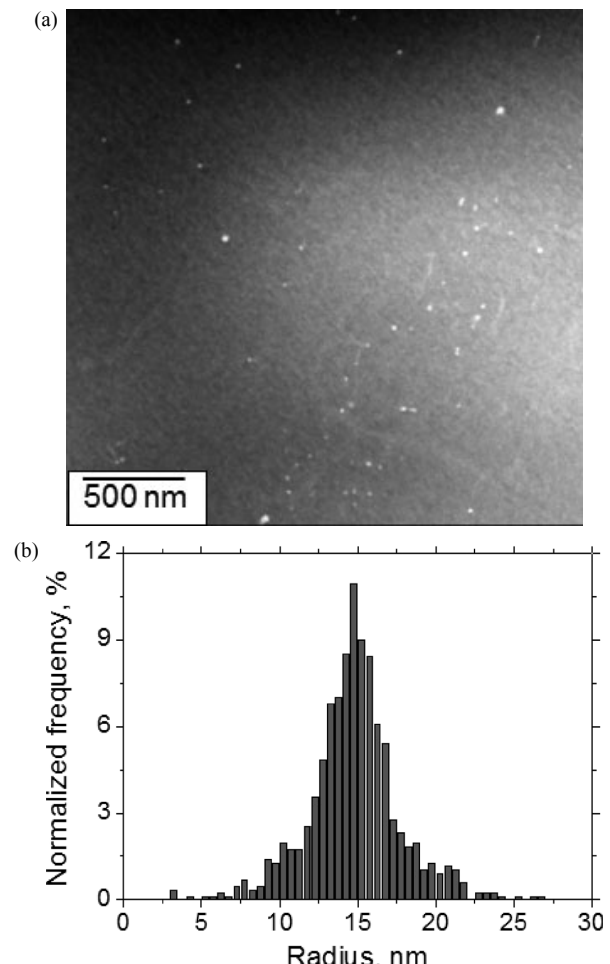


**Fig. 2.** (a) HAADF-STEM image of NbC precipitation and (b) size distribution NbC precipitation in slab.

prior to reheating, with precipitates in the 20–40  $\mu\text{m}$  range. The replica studies combined with electron diffraction confirmed that most of the precipitates of this kind could be positively identified as NbC. A total of 117 particles was analysed to obtain an average radius of  $15.7 \pm 9.9$  nm where the 9.9 nm is the standard deviation of the distribution.

For further quantification of the size distribution of precipitation, high-angle annular dark-field (HAADF) scanning TEM (STEM) images were obtained from the thin foil specimen as shown in Fig. 2(a). Such images exploit atomic number dependent contrast, making them suitable for the statistical treatment of the size distribution using image processing software. In this way, 870 NbC precipitates were examined and the normalised frequency of particle size is presented in Fig. 2(b), with mean size and standard deviation given by  $14.7 \pm 3.0$  nm, comparable to the results from

the carbon replication sample. The size distribution obtained from HAADF images, based on a larger number of particles, was therefore used as an input parameter for the simulation of dissolution behaviour during reheating process.

**Figures 3(a), 3(b)** show the kinetic simulations of the size distribution and phase fraction of NbC precipitates during heating at a rate of  $0.13^\circ\text{C s}^{-1}$ , which is a typical rate during slab reheating. It is interesting that the size distribution and the phase fraction are nearly the same until the temperature reaches to  $1000^\circ\text{C}$ , and the number density, average size and phase fraction of NbC gradually decreases, corresponding to the dissolution process during heating. The changes plotted (Fig. 3(a)) indicate that dissolution dominates any coarsening phenomenon since the mean size of the distribution decreases with an increase in temperature.

Considering the change of equilibrium fraction, however, the kinetic simulation shows a significant deviation from the equilibrium. As shown in Fig. 3(c), the equilibrium phase diagram calculation suggests that a half of NbC precipitates dissolve at  $1000^\circ\text{C}$  and that they are completely decomposed approximately at  $1040^\circ\text{C}$ . On the other hand, the experimental data show that dissolution is far from complete at  $1060^\circ\text{C}$  for the typical slow heating-rate of  $0.13^\circ\text{C s}^{-1}$ . This indicates that kinetics limits the dissolution of NbC in slab, which therefore deviates from any prediction based on equilibrium alone.

To validate the kinetic simulations, the change in the average size of NbC upon heating was examined using interrupted quenching at  $1060$ ,  $1160$  and  $1260^\circ\text{C}$ , respectively. Representative HAADF-STEM images for the precipitation size analysis are shown in Figs. 4(a), 4(b) and the results are summarised in Table 2. A comparison between the calculated and measured mean sizes in Fig. 4(c) shows reasonable agreement, and confirms that NbC dissolution at the heat rate used deviates significantly from that expected under equilibrium conditions. Also Figs. 4(d), 4(e) represent the measured and calculated normalized size distributions of NbC. There is good agreement for  $1060^\circ\text{C}$  but the measured distribution for  $1160^\circ\text{C}$  falls short of that calculated. This is also reflected in the fact that the average size measured for  $1160^\circ\text{C}$  is less than that predicted (Fig. 4(c)). The probable reason for this is that the distribution and average size changes rapidly, as shown in Fig. 4(c), once the temperature exceeds  $1060^\circ\text{C}$ , so that small errors in temperature or homogeneity can have a large effect on the nature of the NbC.

The results shown in Fig. 5 where calculations have been conducted as a function of heating rate are interesting. Naturally, the temperature at which dissolution is complete is reduced as the heating rate becomes slower, but it is also important to note that in the case of the slowest of heating rates studied,  $0.0013^\circ\text{C s}^{-1}$ , substantial coarsening sets in at high temperatures, which is confirmed by experimental observation. It is possible that this could lead to a heteroge-

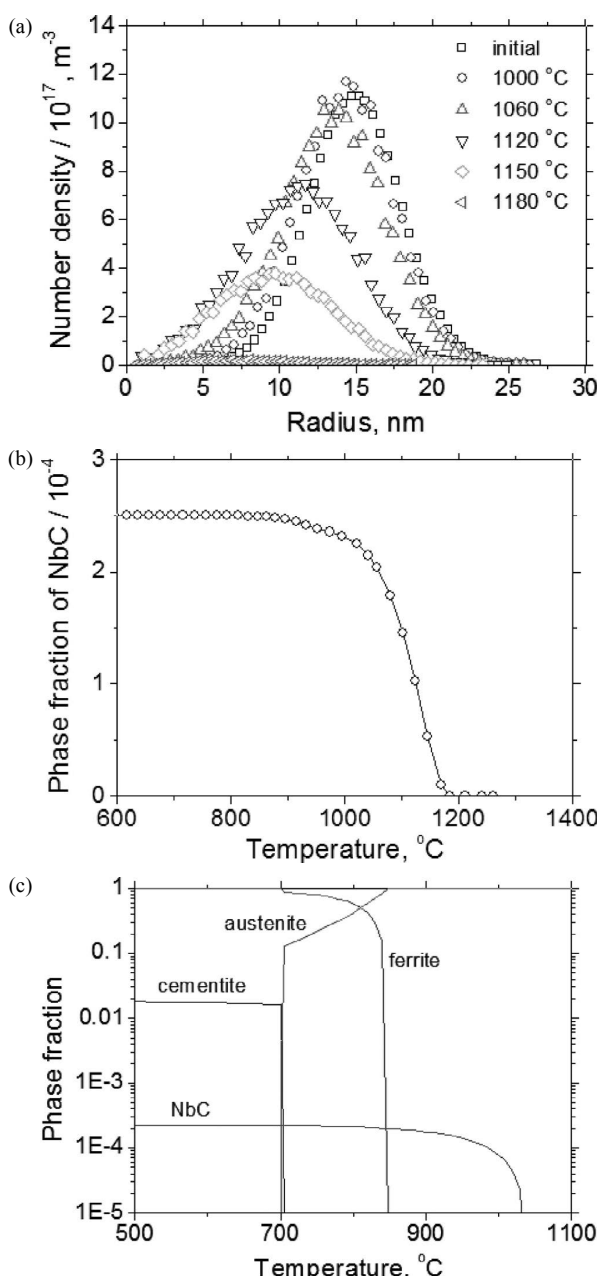
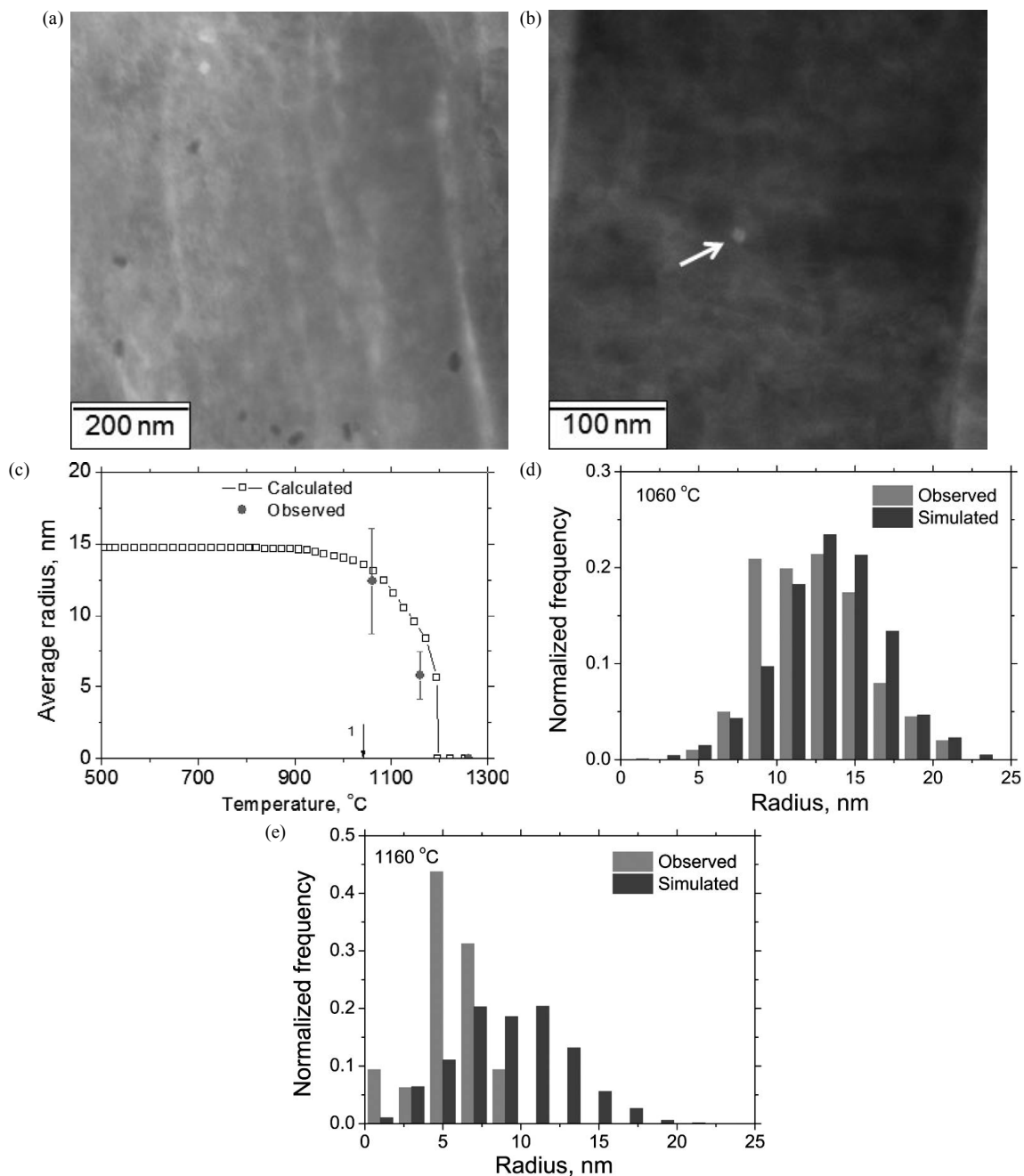


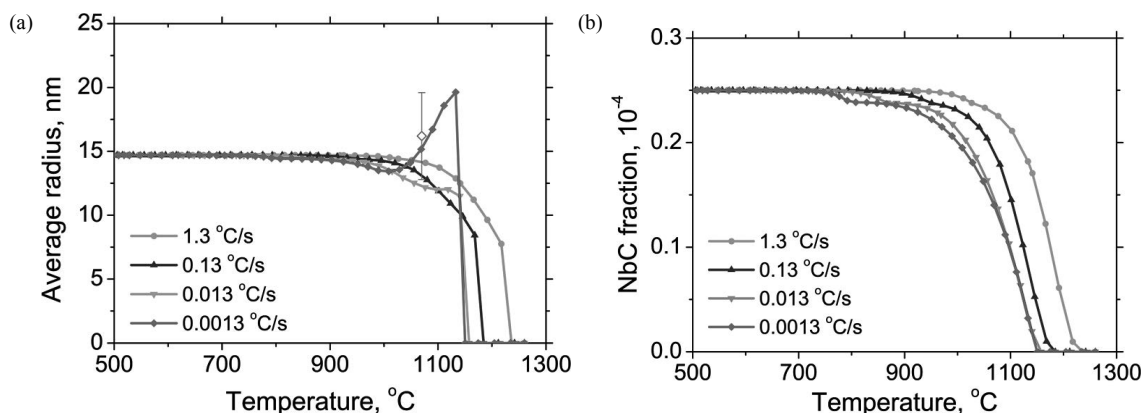
Fig. 3. Calculated (a) number density, (b) phase fraction and (c) equilibrium phase fractions of NbC (using ThermoCalc with TCFE7 database).

Table 2. Average radius of NbC upon reheating.

	$1060^\circ\text{C}$	$1160^\circ\text{C}$	$1260^\circ\text{C}$
Average radius (nm)	$12.4 \pm 3.7$	$5.8 \pm 1.6$	—
Number of precipitates	212	31	0



**Fig. 4.** TEM micrographs showing undissolved NbC (a) at 1060°C and (b) 1160°C. (c) Comparison between calculated and observed radius of NbC upon heating. Arrow indicates the equilibrium temperature for complete dissolution of NbC in the investigated alloy. Comparison between observed and simulated size distribution (d) at 1060°C and (e) 1160°C.



**Fig. 5.** Influence of heating rate on the dissolution behaviour of NbC. (a) mean radius and (b) fraction of NbC. The open symbol in (a) represents the observed average radius at 1170°C at heating rate of 0.0013°C/s.

neous distribution of NbC if the dissolution process is incomplete.

#### 4. Conclusion

The dissolution behaviour of NbC in slab during reheating process is investigated both experimentally and using simulations that have as an input, the experimentally measured initial NbC precipitate size distribution. For a heating rate of  $0.13^{\circ}\text{C s}^{-1}$ , which is typical during slab reheating, the following conclusions can be reached:

(1) The kinetics of dissolution limit the amount of NbC that dissolves less than expected from equilibrium. The kinetic calculation reliably predicts the dissolution kinetics, which is confirmed by microstructural observation using interrupted quenching. It indicates the kinetic consideration is critical for quantitative evaluation of dissolution behavior of NbC during reheating, which is important for the microstructure optimization in subsequent hot-rolling.

(2) Using much slower heating rates has the disadvantage that there is substantial particle coarsening below the temperature at which the volume fraction of NbC becomes zero. This may in some circumstances lead to a small number density of particularly coarse particles surviving in the steel before the hot-rolling process, with potential consequences on the properties of the rolled product.

#### Acknowledgements

The authors are grateful to POSCO for support through Steel Innovation Programme.

#### REFERENCES

- 1) S. Vervynckt, K. Verbeken, P. Thibaux, M. Liebeherr and Y. Houbaert: *ISIJ Int.*, **49** (2009), 911.
- 2) S. Vervynckt, K. Verbeken, B. Lopez and J. Jonas: *Int. Mater. Rev.*, **57** (2012), 187.
- 3) R. Wang, C. Garcia, M. Hua, K. Cho, H. Zhang and A. Deardo: *ISIJ Int.*, **46** (2006), 1345.
- 4) Y. Chen, D. Zhang, Y. Liu, H. Li and D. Xu: *Mater. Charact.*, **84** (2013), 232.
- 5) J. H. Jang, C.-H. Lee, H. N. Han, H. Bhadeshia and D.-W. Suh: *Mater. Sci. Technol.*, **29** (2013), 1074.
- 6) N. Li, L. Li, C. Wang and Z. Wang: *Adv. Mater. Res.*, **712–715** (2013), 65.
- 7) C. Fossaert, G. Rees, T. Maurickx and H. K. D. H. Bhadeshia: *Metall. Mater. Trans. A*, **26A** (1995), 21.
- 8) M. G. Mecoza, J. Sietsma and S. van der Zwaag: *Acta Mater.*, **54** (2006), 1431.
- 9) A. Kundu: PhD Thesis, The University of Birmingham, (2011).
- 10) M. Shome, D. Sharma, O. P. Gupta and O. N. Mohanty: *ISIJ Int.*, **43** (2003), 1431.
- 11) N. Fujita and H. K. D. H. Bhadeshia: *Mater. Sci. Technol.*, **17** (2001), 403.
- 12) P. Maugis, D. Gendt, S. Lanteri and P. Barges: *Defect Diffusion Forum*, **194** (2001), 1767.
- 13) E. Kozechnik, J. Svoboda and F. Fischer: *Calphad*, **28** (2004), 379.
- 14) E. Kozechnik, J. Svoboda, P. Fratzl and F. Fischer: *Mater. Sci. Eng. A*, **385** (2004), 157.
- 15) J. Svoboda, F. Fischer, P. Fratzl and E. Kozechnik: *Mater. Sci. Eng. A*, **385** (2004), 166.
- 16) R. M. Poths, R. L. Higginson and E. J. Palmiere: Institute of Physics Conference Series No. 168 (EMGA), IOP publishing, London, (2001), 201.
- 17) S. Zamberger, M. Pudar, K. Spiradek-Hahn, M. Reischl and E. Kozechnik: *Int. J. Mater. Res.*, **103** (2012), 680.